NTU JOURNAL OF ENGINEERING AND TECHNOLOGY
EISSN: 2788-998X

RESEARCH ARTICLE
Open Access

Natural convection from a radial heat sink with triangular fins

Mohammad S. Hassan[1], Tahseen Ahmad Tahseen[2,*] and Musa M. Weis[3]
{engineer.abosadan@gmail.com[1] tahseen@uokirkuk.edu.iq[2]; musa.weis@ntu.edu.iq[3]}

[1] Mechanical Power Department, Technical College/Kirkuk, Northern Technical University, Iraq
[2] Mechanical Engineering Department, College of Engineering, University of Kirkuk, Iraq
[3] Fuel and Energy Department, Technical College/Kirkuk, Northern Technical University, Iraq
Corresponding author: Tahseen Ahmad Tahseen,email: tahseen@uokirkuk.edu.iq
Co-authors: Mohammad S. Hassan, email: engineer.abosadan@gmail.com
Received: 20-09-2021, **Accepted:** 19-12-2021, **Published online:** 23-02-2022

Abstract. This experimental work dedicated to find the thermal performance of triangular fins in two cases, non-perforated and perforated showing the effect of input factors on the thermal performance. Experiments were carried out by testing three fins for the above two cases and the value of heat input rate with three values: 25.69, 63.58, and 136.9 W. many fixed thermocouples were uesed to measure the temperature in the root of the fin and points along its extension and an additional point to measure the ambient temperature. The Rayleigh number and the Nusselt number were calculated. The effect of the Rayleigh number on the Nusselt number was shown. The results showed that the total heat transfer coefficient of the air increases with the increase in heat added in both cases. In addition, it was found that the temperature decrease along the perforated fin is greater than that of the non-perforated fin, and the total Nusselt number increases with the increase in the heat rate input for both cases. The thermal resistance decreases with the increase in Rayleigh number, both perforated and non-perforated. It was also concluded that the non-perforated fins were more efficient in dissipating heat than the perforated fins, and the reason for this is that the heat transfer was under free convection conditions..

Keywords: Natural convection, triangular fins, radial heat sink, perforated fin.

1.Introduction

The interest has been drawn to the improved of high efficiency electronic devices. This is due to the fact that fossil fuels are running out and global energy consumption is increasing. Moreover, nearly 20% of the global energy is consumed to generate light. For these reasons, traditional lighting devices are being replaced by light-emitting diode (LED) lighting that provids higher efficiency, smaller size and longer life. As lighting devices have been speedily developed over the earlier decades, thermal management, that is, one of the factors for improving the life of lighting devices, is becoming more and more important. Heat sinks were used for the purpose of cooling the LEDs. In the case of LED light bulbs, the photoelectric conversion efficiency is around one-fifth, and the rest of the input energy is released as heat [1,2]. It is recommended to use free convection to cool LED lights, as no additional equipment is required [3-5]. Heat sinks cannot be designed properly, LED lights will reach high temperature and LED lighting life span will be reduced [6-8]. In addition, LED lighting is used in different places and the angle of installation of LED lights can vary according to the usege purpose. The angle of installation is one of the important parameters for cooling LED lighting under free convection. Therefore, it is indispensable to examine cooling performance changes of heat sinks according to the mounting angle with respect to gravity. Not many studies have been conducted on triangular fins compared to plate fins or pin fins regarding the fin geometries of the radial heat sinks. Iyengar and Bar-Cohen [9] studied of the

thermal performance of heat sinks with vertical plate fins, pin fins, or triangular fins attached to a rectangular base under free convection by the least material optimization method. The result shows that the triangular fin heat sink was thermally superior to pin and plate fins in a given environment. Al-Jamal and Khashashneh [10] experimentally studied the effects of pin fins and triangular fins attached to a rectangular base in the case of fixed heat flux, and the Nusselt number correlation obtained from their experimental data showed that the Nusselt number for pin fins was higher than that of triangular fins. Dogan et al. [11] examined the different shapes of fin for a horizontal rectangular base plate by a numerical method, they found that the improved fins showed a higher average coefficient of heat transfer than the plate fins under the same fin area total. However, the geometry of heat sink for these studies cannot be applied directly to LED light, since, in general, the heat sinks for LED light have a circular base with triangular fins placed at regular angular intervals. Recently, several studies have focused on radial heat sink fixed in the circular base to enhance heat dissipation due to the increasing demand for LED lighting applications. Yu et al. [12] examined experimentally the free convection on heat sinks with three types, i.e., L, LM and LMS models, and found that the performance of cooling of the LM model was superior to another models. Costa and Lopes [13] carried out an experimental and numerical study for the thermal performance enhancement of a radial heat sink with a circular base and a spaced rectangular fins number having a central core, using a minimum mass of material. The cooling performance of a radial heat sink with rectangular fins on a circular base has been studied through numerical and experiments by Li and Byon [14]. Lee et al. [15] provided well information on a correlation to predict the Nusselt number for a triangular fin with hollow heat sink to an upper cylindrical base where the applied heat flux in the inner wall of the vertically hollow cylindrical base.

Based on the literature review, there have been few studies on the performance cooling for geometries of heat sink that fit most commercial LED light bulbs, for example, a heat sink with triangular fins and circular base, as shown in Figure 1. The objective of the present work is to investigate the performance of cooling for a radial heat sink with triangular fins on a circular base at various heat flow.

2. Experimental Setup

The experiments were carried out in an experimental facility that was specifically designed and constructed for this purpose. A schematic of this setup is shown in Figure 2. This experimental setup includes a heat sink supplied with heating elements, a data acquisition system, aluminum cylinder and aluminum fins. The heat generated within the heat sink by means of five heating elements each of 50W up to 850W power. All the experimental data are recoded by the data acquisition system. Photographs of this test system as shown in Figures 3.

In the experimental testing using the solid aluminum cylinder with aluminum plate using the fabricated triangular fins. The outer diameter of cylinder is 70 mm and a length of 210 mm. Five holes were made on the upper surface of the cylinder with a diameter of 8 mm and a depth of 200 mm along the length of the cylinder as shown in

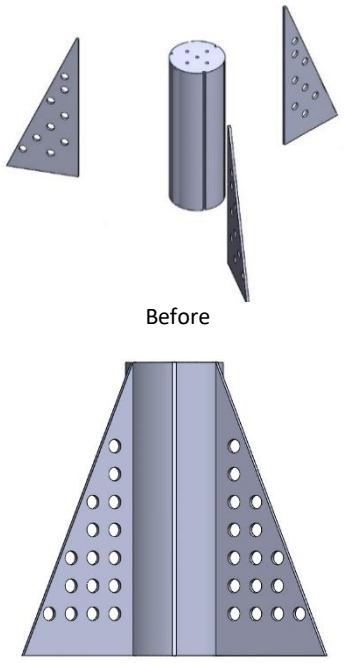

Before

After

Figure 1: The fixed fins on cylinder.

Figure 4 shows a schematic diagram of the cylinder with the all dimensions. Two cases of triangular fins were taken in this study: three fins. The thickness of fin is 3 mm and a length equal to the length of the cylinder is 210 mm and the height of base the triangle is 930 mm, which shows how to install the fins on the cylinder body. Figure 1 shows the fixed fins on base.

The electric power source voltage model HSN 0103, of AC voltage 0-250 V with maximum electric current 5 A. The volt measurement using the volt meter model TENMA9272 the measuring range AC 2v-750. The current measurement using clamp meter model Pro'sKit MT-3102 with the maximum current measuring 400 A. The electric resistors used

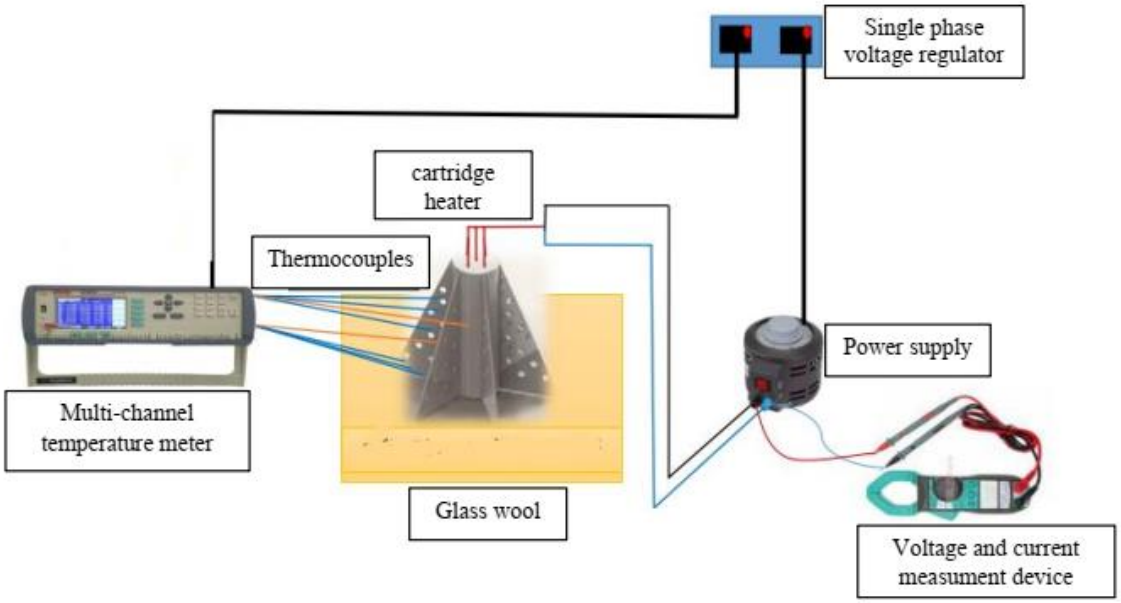

Figure 2: The schematic displayed of the experimental approach.

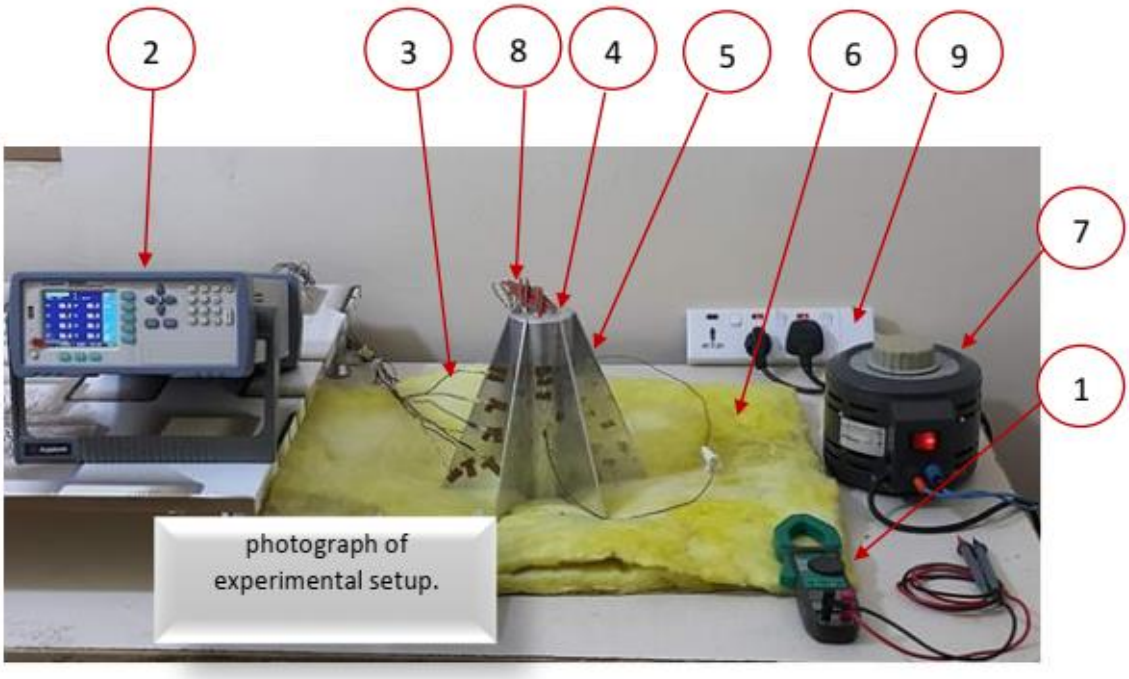

No.	Part Name	No.	Part Name	No.	Part Name
1	Voltage and current measu.	4	Cylinder	7	Single phase voltage regulator
2	Data logger	5	Fin	8	Cartridge heaters
3	Thermocouples	6	Glass wool	9	Power supply

Figure 3: The photograph of experimental setup.

in this work made of circular electric heaters with double step 1000Ω, and the maximum power dissipation of 50 W up to 850 W at 220 V. The outside diameter 8-mm with 200-mm length, electric resistors a small diameter to allow insertion of a cast iron.

For the implementation of temperature measurement a K-type thermoc-ouples has been used. The sensor is based on alteration of the resistivity with temperature and small enough dimensions to not have a great influence on the tests, with operating range -200℃ to 1200℃. Nine thermocouples used to measure temperature, two on cylinder surface, seven on the fin surface with different location and one for measure temperature of room. Figure 5 shows how to fixed thermocouples on cylinder.

The data acquisition with multi-channel temperature meter. The data acquisition model Applent AT4524, with 24 channels temperature recorder meter for industry with LCD display. The thermocouple data logger with the temperature range from -200 ℃ to 1300 ℃ (can see Figure 3).

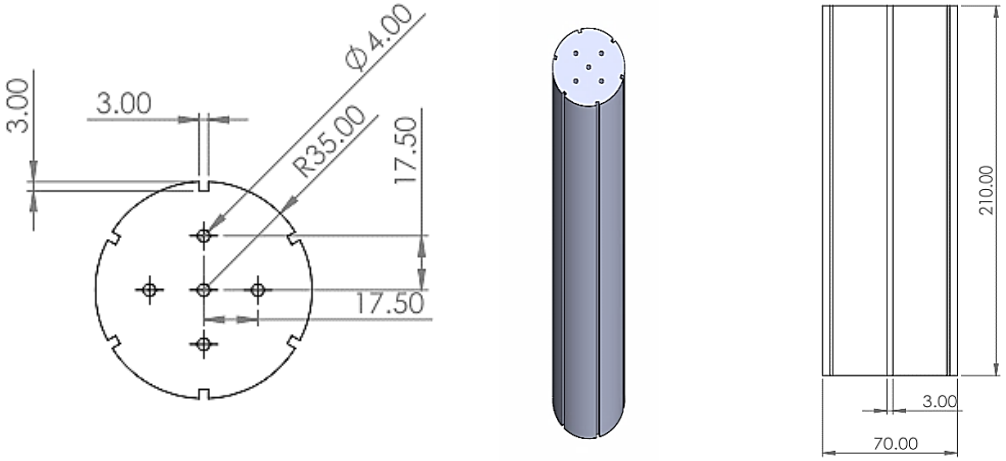

Figure 4: The Schematic diagram of cylinder (all dimension in mm).

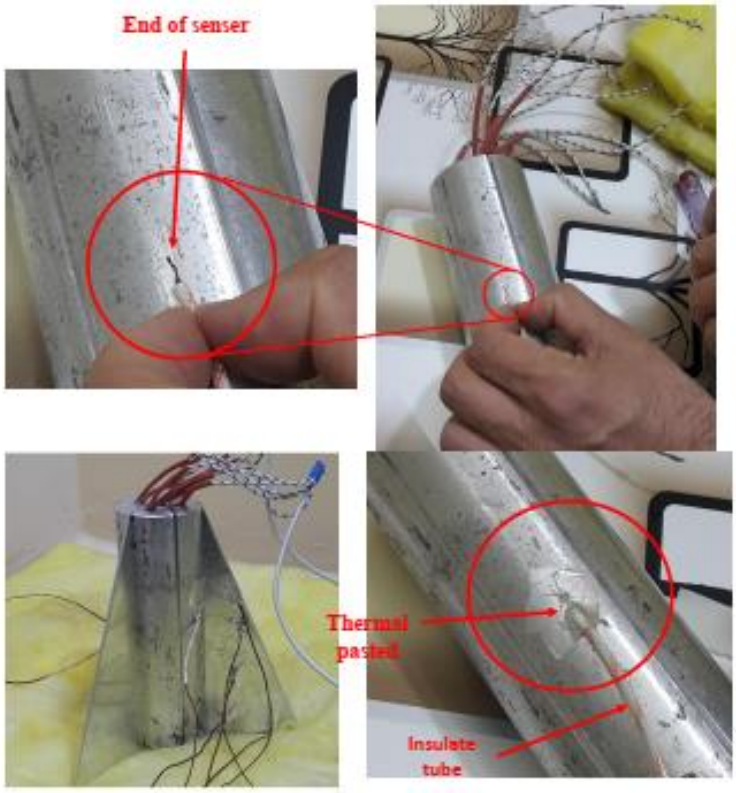

Figure 5: The method of thermocouple fixed on cylinder surface.

3. The Experimental Procedure

Two runs were performed for each experiment. For all experiments, the steady state conditions were reached after 2.5 to 3 hours.
The procedures of the experimental testing for each measurement are as follows:

i. *Electrical power is supplied to the electrical resistance with a voltage of 70 V and current of 0.367A (fixed for all configurations).*
ii. *Approximately 90 min is allowed to pass to balance or equalize the temperatures.*
iii. *The system achieves thermal stability; the condition is then maintained for approximately 90 min.*
iv. *Such stable operation conditions are applied every 90 min to monitor the required values.*

4. Experimental Working Approach

The electrical heat gain rate [voltage (Φ)×current (I)] and uniform heat flux (UHF) from the outer tube surface can be evaluated as:

$$q_{\text{in}} = \Phi \times I \quad \ldots\ldots (1)$$

The steady state heat balance of the electrical heat test surface can be written as:

$$q_{\text{convection}} = q_{\text{in}} - q_{\text{conduction}} - q_{\text{radiation}} \quad \ldots (2)$$

Heat transfer from the system is;

In order to calculate the net heat transfer rate to the heat sink, the heat loss through the Bakelite test section (conduction) is estimated and subtracted from the total power supplied to the heater, the details as follows [14]:

$$Q_{\text{conduction}} = \frac{k_B A_B (T_b - T_B)}{L_B} \quad \ldots\ldots (3)$$

In the experimental study, the maximum heat loss was estimated to be less than 4% of the total heat because of the extremely low thermal conductivity of glass wool is 0.023 W/m oC.
The mean temperature of fin base can calculate by:

$$T_b = \frac{T_{b,1} + T_{b,2}}{2} \quad \ldots\ldots\ldots (4)$$

The rate of heat transfer by radiation was estimated as [16]:

$$Q_{\text{radiation}} = F\sigma A\varepsilon(T_b^4 - T_\infty^4) \quad \ldots\ldots (5)$$

For a commercial aluminium tube with emissivity, $\varepsilon \cong 0.028$, shape factor (F = 0.21) [14]. The experimental error for mean base temperature less than 0.2℃. the loss heat transfer by radiation about 5% form total heat transfer rate because loss emissivity.
The heat flux can calculate as:

$$\dot{Q}_{\text{net}} = \frac{Q_{\text{convection}}}{A_b} \quad \ldots\ldots (6)$$

where (A_b) is the base area fins is defined as the following:

$$A_b = \frac{\pi}{4}D^2 + \pi DL - NLt - 5\left(\frac{\pi}{4}d_{\text{heater}}^2\right) \quad \ldots. (7)$$

where (d_{heater}) electric heat diameter and equal is 8 mm.
The area of fin from the Figure 6 with non-perforated which can be estimated as follows:

$$A_{\text{fin}} = HL + \sqrt{H^2 + L^2}t \quad \ldots\ldots. (8)$$

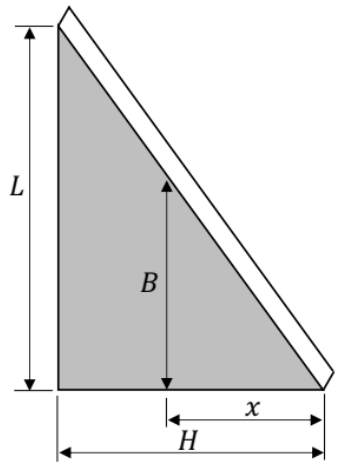

Figure 6. Single triangle fin.

The area of staggered perforated fin can be expressed as follows:

$$A_{\text{fin,per}} = HL + \sqrt{H^2 + L^2}t + 2(n\pi rt - n\pi r^2) \quad \ldots\ldots\ldots (9)$$

where (r) is the drill radius with 5 mm and (n) the number of drill for each fin.
Therefore, the actual heat transfer area can be estimated as follows:

$$A_{\text{act}} = A_b + NA_{\text{fin}} \quad \ldots.(10)$$

$$\left.\begin{aligned}
\rho_{\text{air}} &= 2.209 - 3.414 \times 10^{-3}\left(\frac{T_b + T_\infty}{2}\right), && \text{kg/m}^3\\
\text{C}_{\text{Pair}} &= \left[9.8185 + 7.7 \times 10^{-4}\left(\frac{T_b + T_\infty}{2}\right)\right] \times 10^2, && \text{J/(kg K)}\\
k_{\text{air}} &= \left[3.74152 + 7.495 \times 10^{-2}\left(\frac{T_b + T_\infty}{2}\right)\right] \times 10^{-3}, && \text{W/(m K)}\\
\mu_{\text{air}} &= \left[4.99343 + 4.483 \times 10^{-2}\left(\frac{T_b + T_\infty}{2}\right)\right] \times 10^{-6}, && \text{kg/(m s)}\\
\nu_{\text{air}} &= \frac{\mu_{\text{air}}}{\rho_{\text{air}}}, && \text{m}^2/\text{s}\\
\alpha_{\text{air}} &= \frac{\text{k}_{\text{air}}}{\rho_{\text{air}} \times \text{C}_{\text{Pair}}}, && \text{m}^2/\text{s}\\
\beta_{\text{air}} &= \frac{2}{T_b + T_\infty}, && 1/\text{K}
\end{aligned}\right\} \quad \ldots.(11)$$

The mean free heat transfer coefficient is defined as follows [18]:

$$h = \frac{Q_{\text{net}}}{A_{\text{act}}(T_b - T_\infty)} \quad \ldots.(12)$$

The Nusselt number (Nu) was calculated as follows.

$$Nu = \frac{hL}{k_{\text{air}}} \quad \ldots.(13)$$

The Rayleigh number (Ra) was calculated as follows.

$$Ra = \frac{g\beta_{\text{air}}(T_b - T_\infty)L^3}{\nu_{\text{air}}\alpha_{\text{air}}} \quad \ldots..(14)$$

From the experimental data, the thermal resistance of the heat sink was calculated as follows [15]:

$$R_{th} = \frac{(T_b - T_\infty)}{Q_{net}} \quad \ldots\ldots(15)$$

5. Results and Discussion

The study of the thermal performance of radial triangle non- perforated and perforated fins in this work is presented. The experimental study was conducted through tested for three fins and several points of heat rate supply, with non-perforated and perforated fins which are 25.69 W, 63.58 W and 136.96 W. The following conditions are imposed:

This experiment involves free stream external surface. The following relations for the relevant air properties are used in the following calculations. They are based on data and valid in the range temperature of $275\text{K} \leq 0.5(\overline{T_{in}} + \overline{T_{out}}) \leq 375\text{K}$ [17]:

i. The perforated and non-perforated fins have the same dimensions, namely: L, H and t.
ii. The perforated and non-perforated fins have the same thermal conductivity k.
iii. The base temperature (T_b) for both perforated and non-perforated fins is the same.
iv. The ambient temperature (T_∞) is the same.

As already reviewed in the previous paragraph, many experimental works have been done on non-perforated rectangular fins; the results were usually presented in graphs for the temperature distribution with the fin length, thermal resistance and Nusselt number. Many experiments were carried out to find the base fins temperature distribution in the perforated and non-perforated finned system. The results are presented in Figure 7, the temperature distributions were shown for different heat rates supplied by the

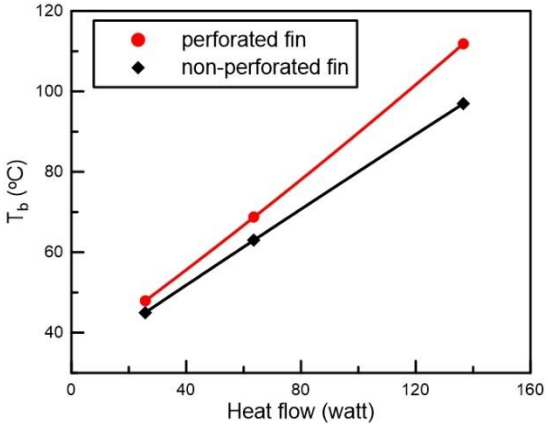

Figure 7: The base fins temperature distribution along perforated and non-perforated fin with various heat supplied.

heating elements. It is clear that the temperature gradient increases as the heat supplied is increased. On the other hand, from the figure shows the upper curve represents a temperature drop in laminar flow region.The second curve shows a differnt behaviors with a sharp drop because it lies near the transition region. The maximum value of the temperature showed in the perforated fins because the air layers contact with many surfaces of fins.

Figure 8 shows the difference between the heat sink base temperature (T_b) and the ambient temperature (T_∞) for various heat inputs (Q) with perforated and non-perforated fin. It can be seen that the temperature difference increases with the heat input for the two cases. The high value of the temperature difference in perforated case due to the various ways of air flow and the increase of the area touch of air layers flow.

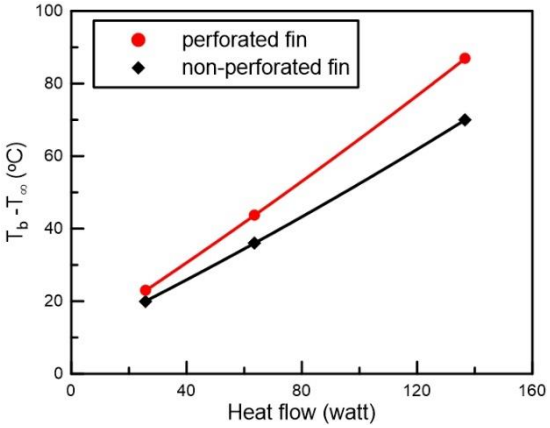

Figure 8: Temperature difference for various perforated and non-perforated fin, and heat inputs.

The fin height is another important parameter that was investigated in the present study. Figure 9 exhibits the impact of the fin height on the temperature distribution along the perforated and non- perforated fins. The studied cases in Figure 9 were for free air flow around and through a fin with nine perforations with heat supplied rate of 25.69 W. As can be noticed in Figure 9, accelerating air around and through a fin delays the air from being heated, which is expected at fixed heat rates. In this way, the temperature difference between the fin and air stays low enough to increase the heat dissipation from the fin. As a result, the fin temperature decreases with increases fin height for two cases. The high value of temperature in perforated fins. The second and third cases of input heat shows in Figures 10 and 11.

Figure 12 shows the effects of design variables on the base temperature for non-perforated fin with different heat inputs. The temperature distribution along the fin has important effect on the fin performance. The base temperature decreases as the fin height increases for all heat input cases due to the increased buoyancy flow. Higher fin temperatures exist as the fin thermal resistance is decreased.

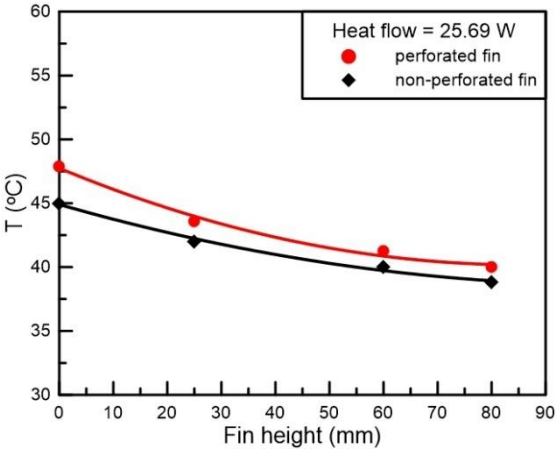

Figure 9: Temperature distribution along perforated and non-perforated fin for heat input 25.69 W.

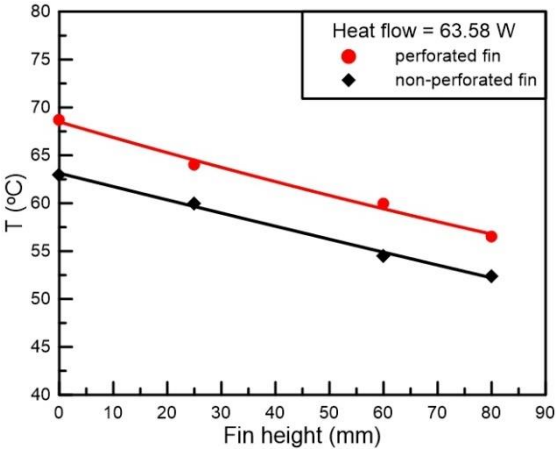

Figure 10: Temperature distribution along perforated and non-perforated fin for heat input 63.58.69 W.

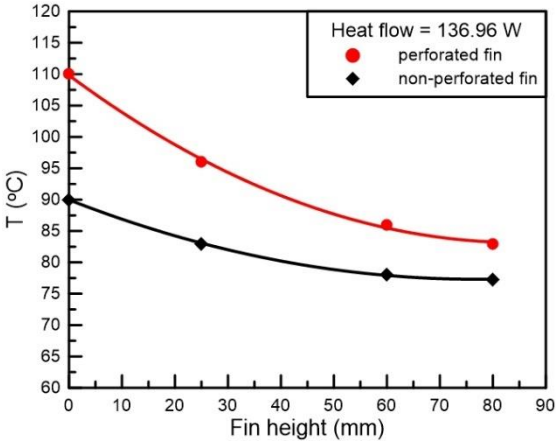

Figure 11: Temperature distribution along perforated and non-perforated fin for heat input 136.96 W.

Figure 13 shows the relationship between the film heat transfer coefficient of the perforated surface and the fin height at different power levels. The film heat transfer coefficient increased with an increase in both the fin height and the input heat.

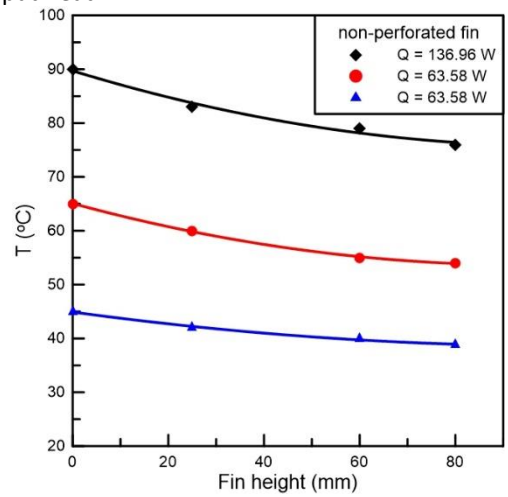

Figure 12: Temperature distribution along non-perforated fin for various heat input.

As shown in Figure 14, as the heat transfer coefficient increases with fin height, the heat transfer coefficient decreases owing to boundary layer overlap and the effective surface area increases as the total surface area increases. As a result, the thermal resistance has its minimum value.

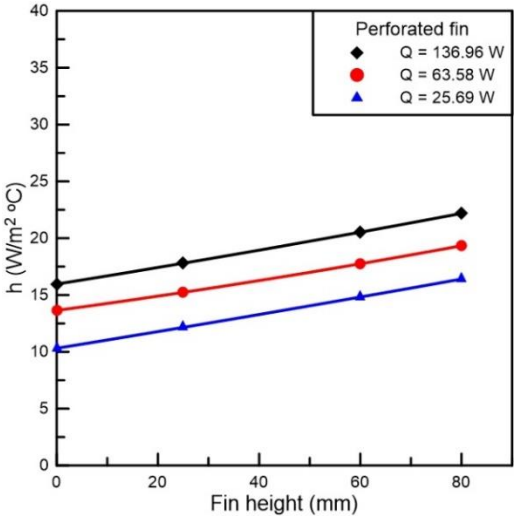

Figure 13: The relationship between heat transfer coefficient and in height at various power levels for perforated fins.

The impact of Rayleigh number on the Nusselt number for perforated and non-perforated fins is shown in Figure 15. It can be seen that; the higher value of Nu is the non-perforated because the heat transfer by free convection.

Figure 16 shows the effects of heat input on the thermal resistance at several heat input at perforated and non-perforated fins. The thermal resistance decreases as the heat transfer rate increases due to the increased buoyancy flow. As shown in Figure 17, the thermal resistance decreases continuously as the Rayleigh number increases for perforated and non-perforated fins. From figure the higher value in perforated fins demonstrates this is because the surface area increases rapidly as the height increases, while the heat transfer coefficient decreases very slowly.

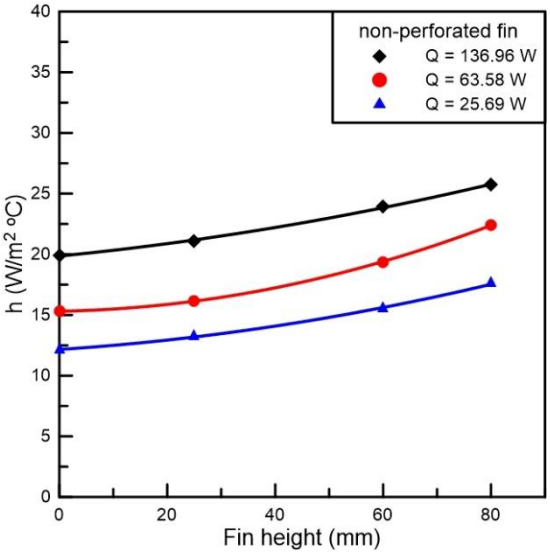

Figure 14: The relationship between heat transfer coefficient and in height at various power levels for non-perforated fins.

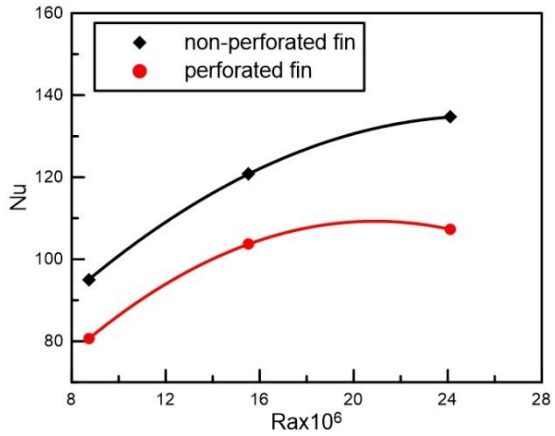

Figure 15: The impact of Rayleigh number on the Nusselt number for perforated and non-perforated fins.

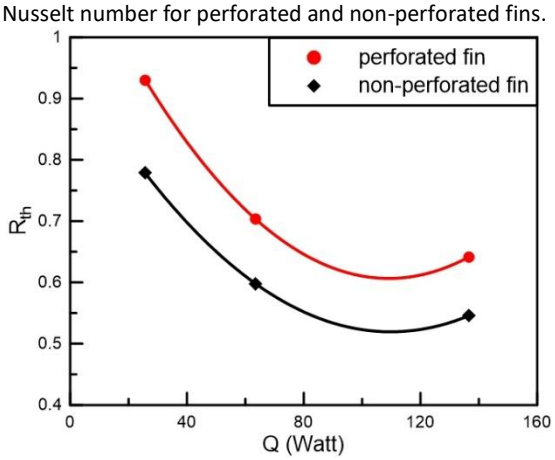

Figure 16: The thermal resistances for various fin height with perforated and non-perforated fins.

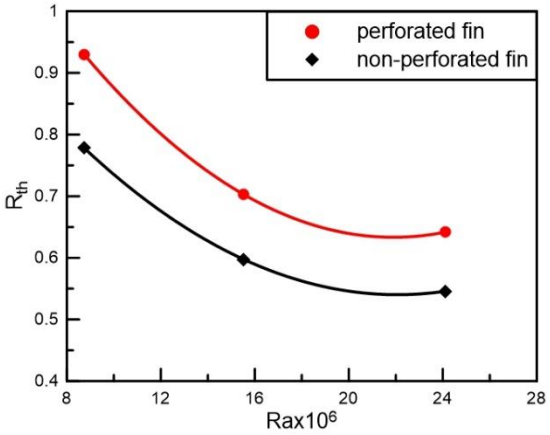

Figure 17: The impact of Rayleigh number on the thermal resistances for perforated and non-perforated fins.

6. Conclusions

The detailed experimental study for free convection in triangular perforated and non-perforated fins with different input heat flow was performed.

Overall heat transfer coefficient of air increases with an increase of input heat value in two studied cases. The overall Nusselt number decreases with an increase of input heat for perforated and non-perforated fins. The temperature drop along the perforated fin length is consistently larger than that for the equivalent non-perforated fin. The thermal resistance decreases continuously as the Rayleigh number increases for perforated and non-perforated fins.

Acknowledgments

The authors would like to thank the Mechanical Power Department, Technical College/Kirkuk, Northern Technical University and College of Engineering, University of Kirkuk for supporting this study.

Nomenclature

A	Area, m^2
Cp	Specific heat capacity, J/(kg ℃)
D	Cylinder diameter, m
g	Gravitational constant, m/s^2
h	Heat transfer coefficient, W/(m^2℃)
H	Height, m
I	Current, A
k	Thermal conductivity, W/(m ℃)
L	Fin length, m
n	Perforation number
N	fins number
Nu	Nusselt number
q	heat flow, W
r	perforation radius, m
Ra	Rayleigh number
R_{th}	Thermal resistance, ℃/W
t	Fin thickness, m
T	Temperature, ℃

Greek symbols

α	Thermal diffusivity, m^2/s
β	Expansion coefficient, 1/K
μ	Dynamic viscosity, kg/(m s)
ν	Kinematic viscosity, m^2/s
ρ	Density, kg/m^3
ε	Emissivity
Φ	Input voltage, V

Subscripts

b	base
B	Bakelite
in	input
∞	ambient

References

[1] Jang, D., Yu, S.-H., and Lee, K.-S. (2012). Multidisciplinary optimization of a pin-fin radial heat sink for LED lighting applications. International Journal of Heat and Mass Transfer, 55(4), 515-521.

[2] Kwak, D.-B., Noh, J.-H., Lee, K.-S., and Yook, S.-J. (2017). Cooling performance of a radial heat sink with triangular fins on a circular base at various installation angles. International Journal of Thermal Sciences, 120, 377-385.

[3] Christensen, A., and Graham, S. (2009). Thermal effects in packaging high power light emitting diode arrays. Applied thermal engineering, 29(2-3), 364-371.

[4] Shen, Q., Sun, D., Xu, Y., Jin, T., Zhao, X., Zhang, N., . . . Huang, Z. (2016). Natural convection heat transfer along vertical cylinder heat sinks with longitudinal fins. International Journal of Thermal Sciences, 100, 457-464.

[5] Huang, G.-J., Wong, S.-C., and Lin, C.-P. (2014). Enhancement of natural convection heat transfer from horizontal rectangular fin arrays with perforations in fin base. International Journal of Thermal Sciences, 84, 164-174.

[6] Wang, J., Zhao, X.-J., Cai, Y.-X., Zhang, C., and Bao, W.-W. (2015). RETRACTED: Experimental study on the thermal management of high-power LED headlight cooling device integrated with thermoelectric cooler package. Energy Conversion and Management, 101, 532-540.

[7] Chiang, K.-T., Chou, C.-C., and Liu, N.-M. (2009). Application of response surface methodology in describing the thermal performances of a pin-fin heat sink. International Journal of Thermal Sciences, 48(6), 1196-1205.

[8] Chen, L., Yang, A., Xie, Z., and Sun, F. (2017). Constructal entropy generation rate minimization for cylindrical pin-fin heat sinks. International Journal of Thermal Sciences, 111, 168-174.

[9] Iyengar, M., and Bar-Cohen, A. (1998). Least-material optimization of vertical pin-fin, plate-fin, and triangular-fin heat sinks in natural convective heat transfer. Paper presented at The intersociety conference on thermomechanical phenomena in electronic systems (ITHERM).

[10] Al-Jamal, K., and Khashashneh, H. (1998). Experimental investigation in heat transfer of triangular and pin fin arrays. Heat and mass transfer, 34(2), 159-162.

[11] Dogan, M., Sivrioglu, M., and Yılmaz, O. (2014). Numerical analysis of natural convection and radiation heat transfer from various shaped thin fin-arrays placed on a horizontal plate-a conjugate analysis. Energy Conversion and Management, 77, 78-88.

[12] Yu, S.-H., Lee, K.-S., and Yook, S.-J. (2011). Optimum design of a radial heat sink under natural convection. International Journal of Heat and Mass Transfer, 54(11-12), 2499-2505.

[13] Costa, V. A., and Lopes, A. M. (2014). Improved radial heat sink for led lamp cooling. Applied thermal engineering, 70(1), 131-138.

[14] Li, B., and Byon, C. (2015). Investigation of natural convection heat transfer around a radial heat sink with a concentric ring. International Journal of Heat and Mass Transfer, 89, 159-164.

[15] Lee, M., Kim, H. J., and Kim, D.-K. (2016). Nusselt number correlation for natural convection from vertical cylinders with triangular fins. Applied thermal engineering, 93, 1238-1247.

[16] Incropera, F. P., Dewitt, D. P., Bergman, T. L., and Lavine, A. S. (2011). Fundamentals of heat and mass transfer (6th ed.). USA: John Wiley & Sons, Inc.

[17] Rogers, G.F.C. and Y.R. Mayhew, Thermodynamic and transport properties of fluids. 5th ed. 2004, UK: Blackwell Publishing.

[18] Bergman, T. L., Lavine, A. S., Incropera, F. P., and Dewitt, D. P. (2011). Introduction to heat transfer (sixth ed.). New York, USA: John Wiley & Sons.